

### <sup>3</sup>He Spin Echo: New Atomic Beam Technique for Probing Phenomena in the neV Range

Maarten DeKieviet, Dirk Dubbers, Christian Schmidt, Dirk Scholz, and Ulrich Spinola

*Physikalisches Institut der Universität Heidelberg, 69120 Heidelberg, Germany*

(Received 20 March 1995)

We have developed a new experimental method for measuring extremely small changes in kinetic energy in a flux of atoms. Analogously to the well-known technique of neutron spin echo, we have succeeded in manipulating the nuclear spins in an atomic beam of <sup>3</sup>He. The result, <sup>3</sup>He spin echo, is a universal, high intensity, high resolution tool for a wide range of areas in physics and molecular sciences. We describe the experimental setup and show first spin echo curves. In addition, we demonstrate the power of the method by resolving a change in energy of the <sup>3</sup>He atoms of ca. 33 neV.

PACS numbers: 39.10.+j, 34.50.-s, 76.60.Lz

In the last few decades atomic and molecular beam techniques have contributed invaluable information in many areas of science [1]. Over the years, especially with the implementation of supersonic expansions, the quality of these beams improved, both in intensity and monochromaticity. In time of flight (TOF) measurements, the latter has determined the energy resolution of scattering experiments performed with atomic and molecular beams. At present, the TOF method seems to have reached a practicable limit of some tenths of meV. In analogy with the spin echo technique used for neutrons [2], we created a new tool for atomic and molecular beam spectroscopies, in which beam monochromaticity no longer limits energy resolution. Since our ultimate goal is to study slow motion in and on surfaces, we chose to develop this method for a helium beam. In the discipline of surface science He scattering has a unique position among all other probes. With thermal beam energies of 10–100 meV, corresponding to de Broglie wavelengths of some Å, a beam of He atoms is exclusively surface sensitive (no penetration into the bulk) and completely inert (no electronic excitations or reactions). Whereas He diffraction reveals structure, inelastic He scattering interrogates the dynamics at or on a surface. For the kind of processes that we will be investigating (diffusion of large molecules, phase transitions, etc.), the energy resolution of standard TOF methods is not sufficient. <sup>3</sup>He spin echo (<sup>3</sup>He-SE) increases this resolution by at least 4 orders of magnitude. In addition, since no chopper is needed, there is a gain in intensity as well, by a factor of 2–100 with respect to TOF.

The basic idea behind <sup>3</sup>He-SE is to use the Larmor precession of the nuclear spin of each <sup>3</sup>He atom as the particle's individual, internal clock. By polarizing the atomic beam, in direction  $x$  perpendicular to the beam axis  $z$ , all clocks get synchronized. At this point the beam averaged polarization  $P_x = 1$ . If we subsequently send the atoms through a magnetic field parallel to the beam, i.e., perpendicular to this macroscopic polarization, of magnitude  $B_1$  and length  $l$ , each nuclear spin will start precessing. The total angle of rotation,  $\phi_1$ , of each spin traversing this spin echo coil with velocity  $v_1$  depends

on the rate of precession, i.e., on the Larmor frequency  $\omega_L = \gamma B_1$ , and the time  $l/v_1$  the atom spends within the magnet:

$$\phi_1 = \gamma \int B_1 dt = \frac{\gamma}{v_1} \int B_1 dl \quad (1)$$

with the gyromagnetic ratio for <sup>3</sup>He,  $\gamma = 2\pi \times 32.433$  MHz/T.

If we start out with a finite width velocity distribution, the atomic beam is no longer polarized at the exit of the SE coil, for spins with different velocities precess over different angles. Exiting the magnet, each clock reads the time that particular particle spent in the SE coil, that is, each precession angle is uniquely linked to a certain velocity through (1).

By applying a second magnetic field  $B_2$  in the opposite direction (i.e., antiparallel to the beam) downstream, we make each <sup>3</sup>He atom precess backward by an angle

$$\phi_2 = -\frac{\gamma}{v_2} \int B_2 dl \quad (2)$$

(we turn back time). If the field integral of the second spin echo coil is identical to the first one and  $v_2 = v_1$ , after having traversed both coils, all nuclear spins point in the  $x$  direction again, for each particle precesses backward by exactly the same angle as it did forward:  $\phi_2 = -\phi_1$ . In general, the point of regained polarization is defined by

$$\left( \frac{d\phi}{dv} \right) = 0 \quad (3)$$

and called the spin echo point. Provided the spin echo field integrals are exactly the same, this condition is met, independent of the magnitude of  $v$ . We may thus explore more of phase space (more intensity) and use atomic beams that have a much larger velocity spread (up to  $\Delta v/v = 20\%$ ) than those required for TOF measurements ( $\Delta v/v < 1\%$ ).

If we detune the SE field integrals, while measuring  $P_x$ , we obtain a spin echo curve of the type presented in Fig. 2. It shows how the <sup>3</sup>He spins dephase by moving away from the spin echo point. Successive maxima indicate multiple revolutions of precession, while the damping is due to the finite width of the velocity distribution

in the beam. Mathematically, the spin echo curve is the cosine transform of the wavelength distribution (with the de Broglie wavelength  $\lambda = h/mv$  as a measure of time):

$$P_x = \langle \cos \Delta \phi \rangle = \gamma \int_{-\infty}^{\infty} f(\lambda) \cos \left[ \frac{\gamma m}{h} \left( \int B_1 dl - \int B_2 dl \right) \lambda \right] d\lambda \quad (4)$$

in which  $m$  stands for the mass of a  $^3\text{He}$  atom,  $f(\lambda)$  represents the wavelength distribution in the beam, and  $h$  is Planck's constant.

If some event, taking place between the spin echo coils (e.g., inelastic scattering), introduces a change in kinetic energy and  $v_2 \neq v_1$ , the  $^3\text{He}$  atoms precess backward by a different amount than they did forward. Each atom leaves the second spin echo coil with an additional phase shift, which, if both spin echo field integrals are equal, amounts to

$$\Delta \phi = \phi_2 + \phi_1 = \frac{\gamma m}{h} (\lambda_2 - \lambda_1) \int B_{1,2} dl. \quad (5)$$

When there are elastic interactions only, the polarization  $P_x$  of a monochromatic, spin polarized beam varies as a function of spin echo coil detuning like a cosine curve. For a beam which suffers a change in kinetic energy, however, the spin echo curve is dispersively shifted with respect to the symmetric case.

We will now discuss some key points in the practical realization of our  $^3\text{He}$  spin echo method; details of the experimental setup will be published elsewhere. Schematically, the  $^3\text{He}$ -SE apparatus consists of the following sequence of elements (see Fig. 1): (a) an atomic beam source, (b) a polarizer, (c) a guide field, (d) a first SE coil, (e) a second SE coil, (f) a guide field, (g) an analyzer, and finally (h) a detector.

Since the magnetic moment of the  $^3\text{He}$  nuclear spin is rather small, we have to apply quite intense, inhomogeneous magnetic fields in order to spin polarize and spin

analyze our atomic beam. The residence time within these Stern-Gerlach type magnets increases by reducing the kinetic energy of the helium atoms. With a temperature of the liquid  $^4\text{He}$  cooled nozzle source of 1.3 K, we obtain a beam energy of less than 0.3 meV, which corresponds to an atomic velocity of less than 100 m/s. For initial spin selection, we use a ca. 0.4 m long electromagnetic quadrupole field with more than 1 T at the pole shoes. A permanent sextupole analyzer of comparable length and strength selects the final spin state entering the detector.

In neutron spin echo (NSE) experiments, the nonadiabatic spin state transitions between guiding fields and SE fields, and in between SE fields (referred to as  $\pi/2$  and  $\pi$  flips, respectively), can be realized easily using so-called Mezei coils. Since  $^3\text{He}$  atoms, in contrast with neutrons, do not penetrate through matter at all, we used a sequence of magnetic fields separated by zero-field regions. This scheme for flipping spins has been successfully implemented earlier, both in NSE experiments (related to a search for neutron-antineutron oscillations [3]), and in an atomic beam experiment (on manipulating the electron spin of lithium [4]). In short, a nonadiabatic transition between two magnetic fields is achieved by exponentially decreasing the magnitude of the first down to a level at which the corresponding Larmor frequency  $\omega_L$  of spins traversing this field is less than the angular velocity  $\omega_B$  of the field, as seen by the moving particle. Coarsely speaking, the spins must practically stop noticing the presence of the first magnetic field before they are to feel the second. The latter then grows from  $\omega_L \ll \omega_B$  to  $\omega_L \gg \omega_B$ . This method for flipping spins thus requires relatively long regions of extremely low magnetic background ( $B_{\text{Background}} < 100$  nT, "zero field"). We achieve this by enclosing the entire beam path with a doubly layered mu-metal shield, which from time to time can be demagnetized. In this manner we are able to produce  $\pi/2$  flips between the guiding fields and the SE coils to within  $3^\circ$ , and a  $\pi$  flip between both SE fields to better than  $4^\circ$  of dephasing.

The actual spin echo coils have been constructed following the optimal Larmor precession field shape of Zeyen *et al.* [5]. This design has the advantage that off-axis field integral inhomogeneities in a spin echo coil are minimal (the magnetic field intensity varies as a half wave of  $\cos^2$  along the beam axis). The two spin echo coils used in our experiment each produce the same magnetic field integral of 2.34 mTm per ampere coil current to better than  $10^{-4}$  within the beam diameter of 6 mm. On top of the second, we wound another  $\cos^2$  coil with a slightly lower integral value of 1.99 mTm/A. This so-

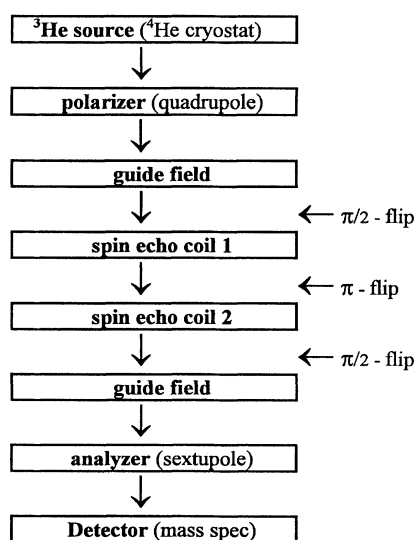


FIG. 1. Schematic representation of the  $^3\text{He}$ -SE spectrometer.

called  $\Delta B$  coil allows us to detune the total magnetic field integral about the spin echo point.

The spin echo curve shown in Fig. 2(a) is for the special case of  $B_1 = B_2 = 0$ , i.e., with no current through the spin echo coils (and therefore rather called a spin dephasing curve). The combined efficiencies of polarizer and analyzer determine the value of the global maximum of this curve, which corresponds to an overall polarization product of 90%. In general, the net polarization at the spin echo point decreases only moderately with increasing spin echo field strength. For example, using spin echo field integrals in which the  $^3\text{He}$  spins precess some 3000 times forward and 3000 times backward, we still achieve 40% polarization. From the period of the oscillations in Fig. 2(a), we determine via (4) the average velocity of the  $^3\text{He}$  atoms (in this particular example 151 m/s).

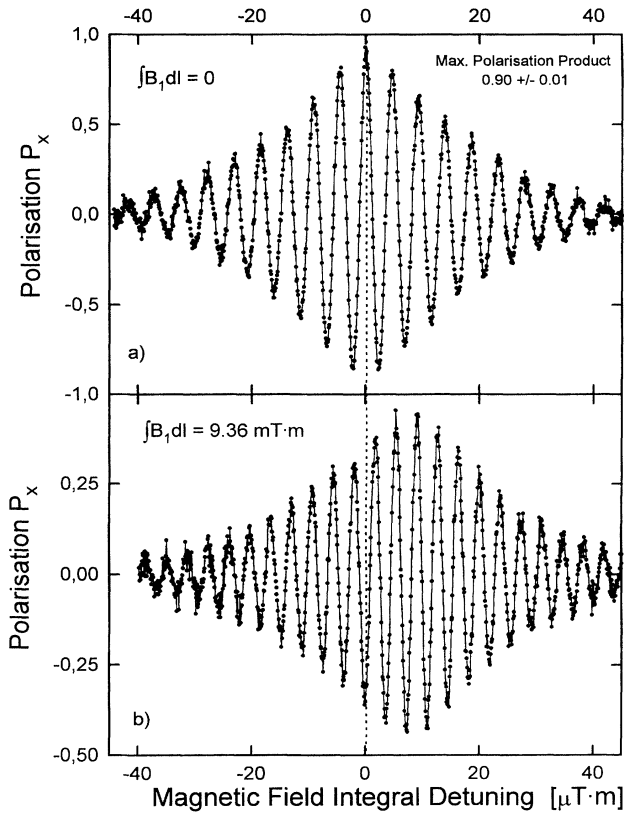


FIG. 2. (a) The spin rotation curve is obtained by monitoring the count rate at the detector, while detuning using the  $\Delta B$  coil around the symmetric field constellation  $B_1 = B_2 = 0$ . The center maximum of this curve represents the overall polarization efficiency of the apparatus and amounts here to almost 90%. (b)  $^3\text{He}$  spin echo curve taken with the inclined setup. Both spin echo coils are set to produce a magnetic field integral of 9.36 mT·m each, which causes the nuclear spins to precess some 3000 revolutions in each direction. Note that the entire spin echo group is shifted with respect to  $\Delta B = 0$ . This is due to the loss of ca. 33 neV of kinetic energy by the  $^3\text{He}$  atoms flying against gravity. The asymmetry in the envelope of the spin echo curve is a measure of dispersion caused by this fixed energy loss.

The width of the velocity distribution in the beam, here  $\Delta v/v \approx 10\%$ , causes damping of this curve. In Fig. 3 (dots) we compare a measured TOF spectrum with one (solid line) acquired by taking the cosine transform of the spin echo curve in Fig. 2(a).

As a quick and physically simple demonstration of the ability of this method to measure small changes in kinetic energy, we ramped the entire apparatus (overall length ca. 6 m) to an inclination of 10%. In this configuration, gravity introduces a difference between the two angles of precession in the first and the second spin echo coil, through two different processes. At first, the  $^3\text{He}$  atoms, flying uphill towards the detector, gain gravitational energy between the centers of the spin echo coils (height difference  $\Delta h = 10.9$  cm), thus losing a fixed amount of kinetic energy:

$$\Delta E = mg\Delta h \approx 33 \text{ neV}. \quad (6)$$

This energy difference corresponds to a difference in atom velocities before and after the  $\pi$  flip, and thus leads to an additional phase shift in the spin echo curve,

$$\Delta\phi \propto \lambda^3. \quad (7)$$

Explicitly, this shift in precession angle is measured as an offset in the  $\Delta B$  coil:

$$\int \Delta B dl = \frac{\Delta E m}{h^2} \lambda^2 \int B_0 dl. \quad (8)$$

In Fig. 2(b) we show a spin echo curve taken with this inclined setup; notice a shift of the spin echo curve with respect to  $\Delta B = 0$ . Keeping everything else the same ( $B_0$ ,  $\Delta\lambda/\lambda$ , and  $\Delta E$ ), we measured this shift as a function of  $\lambda$ , the mean wavelength of the beam (see Fig. 4). We were able to vary the latter by changing the current through our quadrupole polarizer, which, through focusing, has velocity selecting properties as well. Within

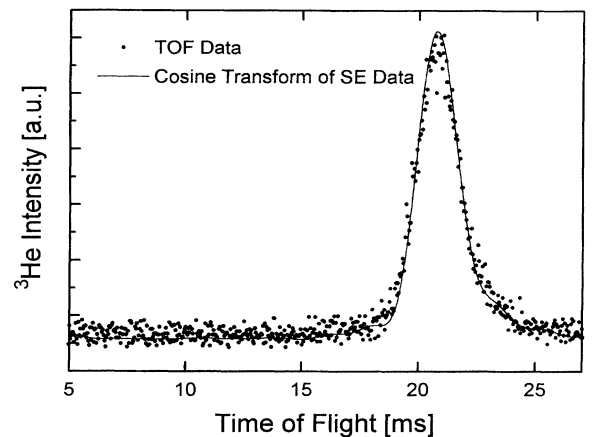


FIG. 3. The solid line shows the TOF spectrum deduced from the spin rotation curve in Fig. 2(a). Mathematically, the spin rotation curve is the cosine transform of wavelength distribution of the beam, and thus contains equivalent information. This is visualized by the dots in this figure, which represent measured TOF data.

the limited tuning range under these conditions, the curve in Fig. 4 shows the quadratic dependency described by (8). There is no physical process of lower order in  $\lambda$ . The best fit through the data (the solid line in Fig. 4) contains a quadratic term only. It shows, however, a coefficient that is some 50% larger than that following from (8). This is due to gravity as well, but via a second mechanism.

For the very slowly moving  $^3\text{He}$  atoms, gravity causes the particles' trajectories to deviate noticeably from a simple straight line. An atom traversing a parabolic trajectory samples a slightly different magnetic field integral, which depends on its wavelength, in each of the SE coils. This effect can be neglected for a perfectly aligned apparatus. However, by ramping up the end of the apparatus by ca. 0.6 m, the two spin echo coils may have become not exactly concentric around the (well defined and aligned) beam path. Under normal conditions (horizontal setup) this would merely lead to an offset of the spin echo curve, and thus a constant contribution to the curve in Fig. 4, independent of  $\lambda$ . In the inclined experiment, however, gravity causes  $\lambda_2 \neq \lambda_1$ , and there is a second order effect of the misalignment, giving an additional quadratic contribution. From Fig. 4 we determine the center of one spin echo coil to be ca.

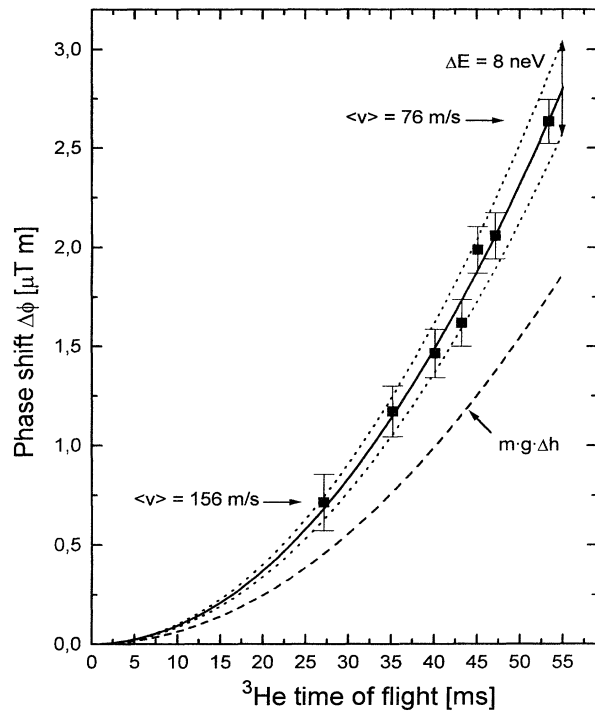


FIG. 4. Plot of the phase shift of a spin echo group, determined from spin echo curves of the type in Fig. 3, as a function of the average  $^3\text{He}$  beam velocity. The solid line is a quadratic fit (no linear terms) based on (8). The parabolic contribution caused by the  $m\mathbf{g}\Delta h$  gravity term only is plotted as well.

1.5 mm lower than the beam axis. It is important to note, however, that the observed gravity effect in Fig. 4 cannot be totally due to misalignment, for that would require one spin echo coil to be off center by at least twice the beam radius, which is physically impossible.

Although in the prospective use of the apparatus as a spectrometer this systematic effect is irrelevant, we have reduced the origin of this misalignment and have resumed normal (i.e., horizontal) operation conditions. The resolution of our method therefore is determined by the error bars in Fig. 4, which are statistical in nature. In conclusion, we thus claim that with  $^3\text{He}$ -SE we are able to resolve changes in kinetic energy on the order of 15 neV or less.

We are now in the process of adding surface science capabilities to this  $^3\text{He}$  spectrometer. At the point of the  $\pi$  flip, i.e., in the middle between the two SE coils, we are constructing a nonmagnetic, UHV scattering chamber with a cryogenic crystal manipulator. It will become the center of rotation for both the crystal and the detector (or better, for everything downstream from the  $\pi$  flip). Therewith, we can select the exact kinematic conditions of the atom-surface interaction, i.e., the momentum exchange  $\vec{q}$ .  $^3\text{He}$ -SE then allows us to measure the time correlation function  $I(\vec{q}, t)$  of the 2D system directly, without any model dependent assumptions [2].  $I(\vec{q}, t)$  is the Fourier transform in time of  $S(\vec{q}, \Delta E = \hbar\omega)$ , the scattering function obtained by traditional techniques. The discussed energy resolution of 15 neV thus opens the possibility for studying correlations in surface scattering experiments on long time scales, up to  $10^{-8}$  s.

We are indebted to Professor Dr. E. Steffens, from the Max Planck Institut für Kernphysik in Heidelberg, for lending us both the polarizing and analyzing multipole magnets. In addition, we would like to thank him and Professor J.P. Toennies, from the Max Planck Institut für Strömungsforschung in Göttingen, for the detailed discussions we had in early stages of the experiment. Finally, we thank S. Urlich for his help during the measurements.

- 
- [1] G. Scoles, *Atomic and Molecular Beam Techniques* (Oxford Press, New York, 1992); J.P. Toennies, *Surface Phonons*, edited by W. Kress and F.W. de Wette, Springer Series in Surface Science Vol. 21 (Springer, Berlin, 1991), p. 111.
  - [2] F. Mezei, *Int. J. Mod. Phys.* **B7**, 2885 (1993), and references therein.
  - [3] U. Schmidt, T. Bitter, P. El-Muzeini, D. Dubbers, and O. Schärpf, *Nucl. Instrum. Meth. Phys. Res., Sect. A* **320**, 569 (1992).
  - [4] W. Schröder and G. Baum, *J. Phys. E* **16**, 52 (1983).
  - [5] C.M.E. Zeyen, P.C. Rem, R.A. Hartmann, and L.J.M. van de Klundert, *IEEE Trans. Magn.* **24**, 1540 (1988).